

NEUROPROTECTION BY DIHYDROGINSENSOSIDE Rb1

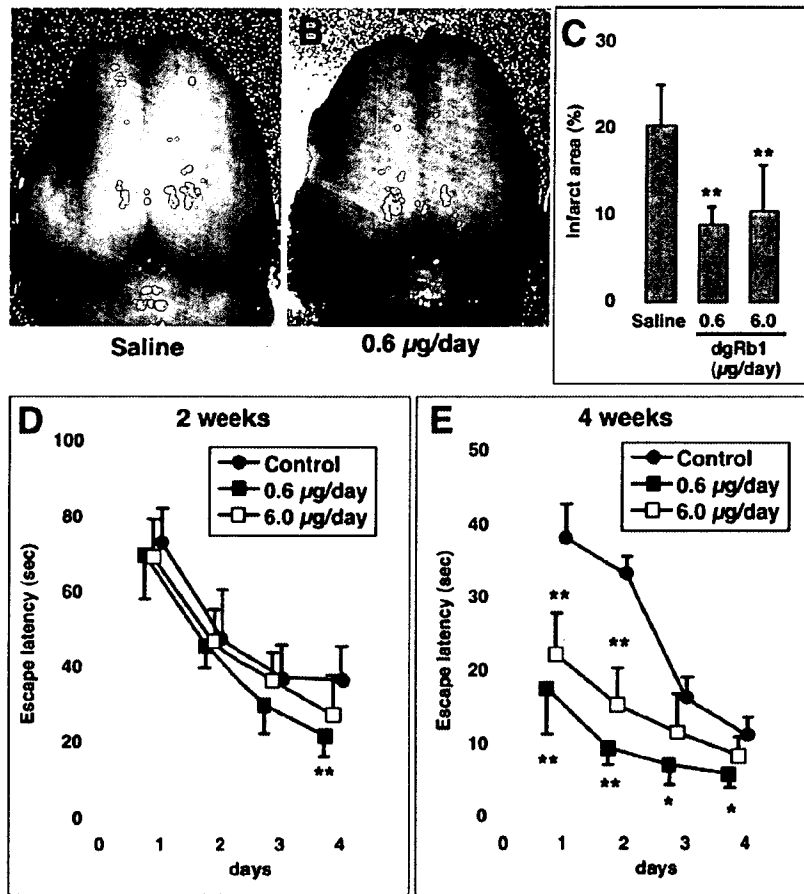


FIG. 7. Intravenous infusion of dihydrogensenoside Rb1 (dgRb1) ameliorated place navigation disability and cortical infarct size in stroke-prone spontaneously hypertensive rats (SHR-SP) at 4 weeks after permanent middle cerebral artery occlusion (MCAO). (A,B) Photomicrographs showing cortical infarct in vehicle-infused rat (A) and dgRb1 (0.6 µg/day)-infused rat (B) with permanent MCAO. (C) Effect of posts ischemic intravenous dgRb1 infusion on ratio of infarcted area to contralateral hemispheric area. Note that dgRb1 at doses of 0.6 and 6.0 µg/day significantly reduced the infarct ratio (%; $n = 6$ in each group). (D,E) Morris water maze tests carried out at 2 weeks (D) and 4 weeks (E) after MCAO in SHR-SP that received intravenous infusion of either vehicle (saline) or dgRb1 (0.6 or 6.0 µg/day; $n = 6$ in each group). Note that dgRb1 at 0.6 µg/day significantly decreased the escape latency on repeated trials of the Morris water maze test, especially on the fourth trial day at 2 weeks after MCAO and on all four trial days at 4 weeks after MCAO. ***Significantly lower ($p < 0.05$, $p < 0.01$, respectively) than saline-treated control.

increase in VEGF protein expression and a 1.6-fold increase in Bcl-x_L protein expression in cortical neurons (Fig. 10B,C).

Induction of VEGF mRNA by dgRb1 Is Dependent on HRE

To determine whether induction of VEGF mRNA by dgRb1 is actually dependent on transactivation of hypoxia response element (HRE), we constructed VEGF promoter-luciferase plasmids carrying wild-type HRE

(VEGF-wt) or mutant HRE (VEGF-mut), and a plasmid that does not carry HRE (VEGF-short). Primary cultured neurons were transfected with these promoter-reporter plasmids and incubated for 24 h in the presence or absence of dgRb1 (1 fg/mL). Then, luciferase activity in the cell lysate was assayed. Experiments were performed five times independently. As a result, relative luciferase activity in dgRb1-treated neurons was significantly higher than that in vehicle-treated neurons when the cells were transfected with VEGF-wt plasmid (1.9-fold; $p < 0.01$; Fig. 11A). When VEGF-mut or VEGF-short plas-

TABLE 1. PHYSIOLOGICAL PARAMETERS BEFORE, DURING, AND AFTER MIDDLE CEREBRAL ARTERY OCCLUSION

Time after MCAO	Vehicle control group	dgRb1-treated group (6 μ g/day)
Mean arterial blood pressure (/min)		
Before	198 \pm 13	204 \pm 20
0 h	194 \pm 14	193 \pm 11
2 h	201 \pm 14	196 \pm 13
4 h	204 \pm 16	197 \pm 10
8 h	195 \pm 14	196 \pm 15
12 h	203 \pm 11	199 \pm 12
24 h	199 \pm 15	205 \pm 14
Brain temperature ($^{\circ}$ C)		
Before	37.3 \pm 0.1	37.3 \pm 0.1
0 h	37.2 \pm 0.1	37.2 \pm 0.2
2 h	37.2 \pm 0.1	37.2 \pm 0.3
4 h	37.4 \pm 0.3	37.6 \pm 0.4
8 h	37.7 \pm 0.2	37.7 \pm 0.2
12 h	37.7 \pm 0.2	37.8 \pm 0.3
24 h	37.8 \pm 0.4	37.8 \pm 0.3

dgRb1, dihydroginsenoside Rb1; MCAO; middle cerebral artery occlusion.

Data are represented as means \pm SD. $n = 6$ in each group. There are no significant differences between two groups.

mid was used for transfection, there was no significant difference between dgRb1-treated neurons and untreated neurons (Fig. 11A). These findings indicate that hypoxia response element on the VEGF promoter is responsible for the induction of VEGF mRNA by dgRb1 in cultured neurons.

Induction of *bcl-x_L* mRNA by dgRb1 Is Dependent on STRE

To confirm that dgRb1-induced *bcl-x_L* mRNA expression is dependent on transactivation of Stat5 response element (STRE), we also constructed *bcl-x* promoter-luciferase plasmids carrying wild-type STRE or mutant STRE (*bcl-x-mut*), and a plasmid that does not carry STRE (*bcl-x-0.6L*). Primary cultured neurons were transfected with these promoter-reporter plasmids and incubated in the presence or absence of dgRb1 (1 fg/mL). One day later, dual luciferase assay was carried out. Data were obtained from five independent experiments. Consequently, relative luciferase activity in dgRb1-treated neurons was significantly higher than that in vehicle-treated neurons when the cells were transfected with *bcl-x-wt* plasmid (2.0-fold, $p < 0.01$; Fig. 11B). On the other hand, when *bcl-x-mut* or *bcl-x-0.6L* plasmid was used for transfection, there was no significant difference between dgRb1-treated neurons and untreated neurons (Fig. 11B). These results suggest that STRE on the *bcl-x_L* promoter is responsible for the induction of *bcl-x_L* mRNA by dgRb1 in cultured neurons.

DISCUSSION

In the present study, we dehydrogenated gRb1 and produced dihydroginsenoside Rb1 (dgRb1), a stable chemical derivative of gRb1. DgRb1 was expected to be effective at a lower dose, compared with gRb1. As we expected, dgRb1 showed protective effects on ischemic brain damage at an approximately ten times lower dose than gRb1 (Zhang et al., 2006). Furthermore, we showed that intravenous infusion of dgRb1 ameliorated SCI as well as ischemic brain damage.

The pathological sequelae after SCI are divided into two broad chronological events: primary injury and secondary injury (Profyris et al., 2004). Primary injury is caused by direct mechanical trauma to the spinal cord where focal destruction occurs. This initial injury is followed by secondary injury. A series of processes in secondary injury including ischemia, edema, revascularization and inflammation is thought to enlarge the area of cell death through necrosis and apoptosis (Beattie, 2004). Among them, ischemia has been demonstrated as to be a crucial factor in post-injury pathophysiological changes in acute SCI, because it is believed to aggravate secondary injury and to occur parallel to neurological dysfunction. Revascularization is also an important factor to regain blood flow in the ischemic tissue. Secondary injury of the spinal cord declined along with revascularization of the involved tissue (Zhang and Guth, 1997). This evidence suggests that revascularization precedes

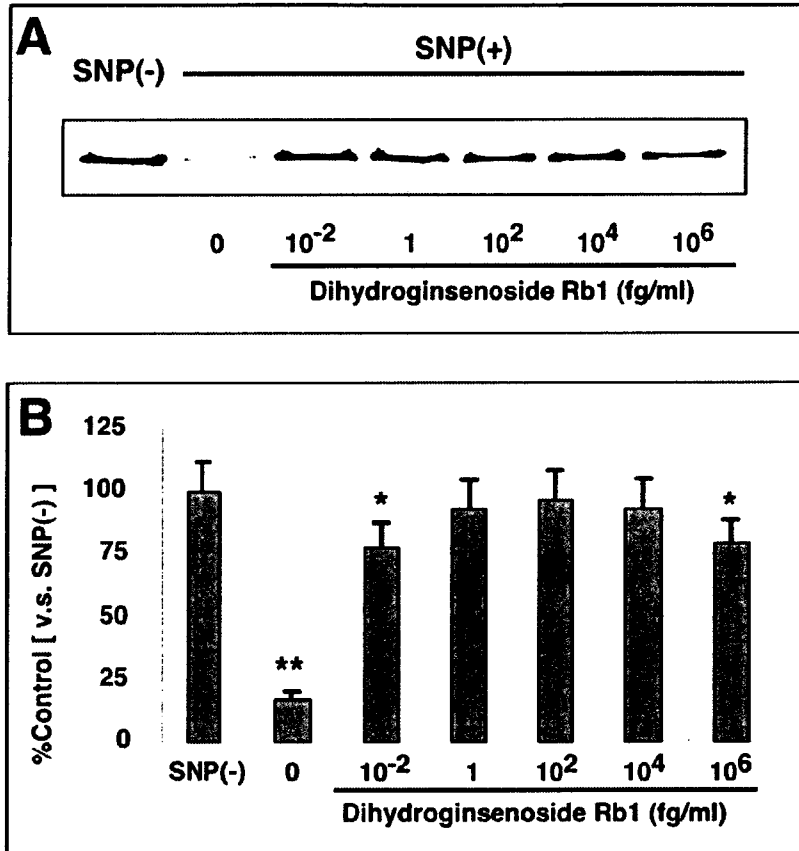


FIG. 8. Dihydroginsenoside Rb1 (dgRb1) prevented NO-induced neuronal apoptosis. (A) Immunoblot analysis of MAP2 protein expression in cultured cortical neurons 16 h after 100 μ M SNP treatment in the presence of 0–10⁶ fg/mL dgRb1. (B) Densitometric analysis of MAP2-immunoreactive bands revealed that MAP2 protein expression in cortical neurons treated with SNP in the presence of 1, 100, or 10,000 fg/mL dgRb1 was maintained at a level close to that of control cortical neurons without SNP treatment. Data were obtained from five independent experiments. ***Significantly lower ($p < 0.05$, $p < 0.01$, respectively) than control without SNP treatment.

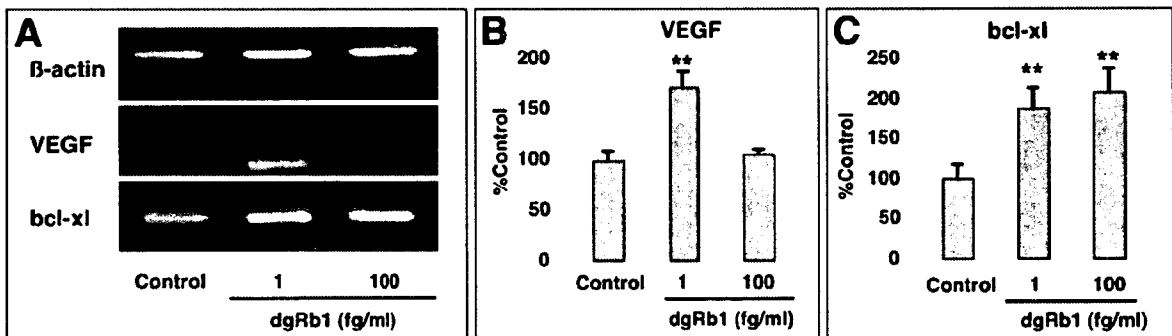


FIG. 9. Dihydroginsenoside Rb1 (dgRb1) upregulated VEGF and bcl-x_L mRNA expression in neurons. (A) Representative photographs of RT-PCR for VEGF and bcl-x_L mRNA in cortical neurons cultured for 24 h in the presence of 0, 1, or 100 fg/mL dgRb1. β -actin was also amplified as an internal control from each sample. (B,C) Densitometric analysis of mRNA levels of VEGF (B) and bcl-x_L (C) in neurons incubated with 0, 1, or 100 fg/mL dgRb1 for 24 h. Data were obtained from five independent experiments. Note that VEGF mRNA expression was upregulated by treatment with dgRb1 at a concentration of 1 fg/mL. Expression of bcl-x_L mRNA was also upregulated by treatment with dgRb1 at concentrations of 1 and 100 fg/mL. **Significantly higher ($p < 0.01$) than vehicle-treated control.

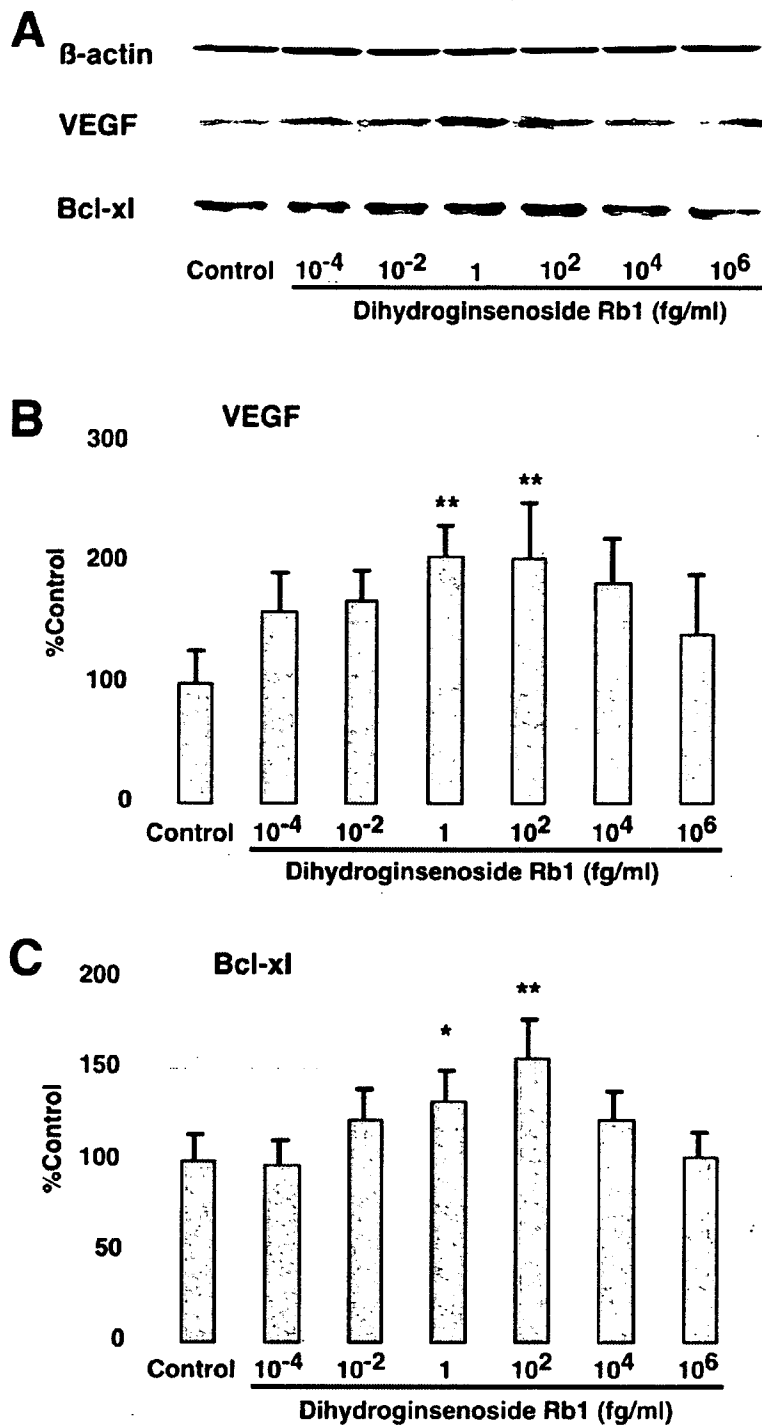


FIG. 10. Dihydroginsenoside Rb1(dgRb1) upregulated VEGF and Bcl-x_L protein expression in neurons. (A) Representative photographs of Western blot for VEGF and Bcl-x_L protein in cortical neurons cultured for 48 h in the presence of 0–10⁶ fg/mL dgRb1. β -actin was used as an internal control from each sample. (B,C) Densitometric analysis of VEGF (B) and Bcl-x_L (C) immunoreactive bands in neurons incubated with 0–10⁶ fg/mL dgRb1 for 48 h. Data were obtained from five independent experiments. Note that VEGF and Bcl-x_L protein expression were upregulated by treatment with dgRb1 at concentrations of 1 and 100 fg/mL. ***Significantly higher ($p < 0.05$, $p < 0.01$, respectively) than vehicle-treated control.

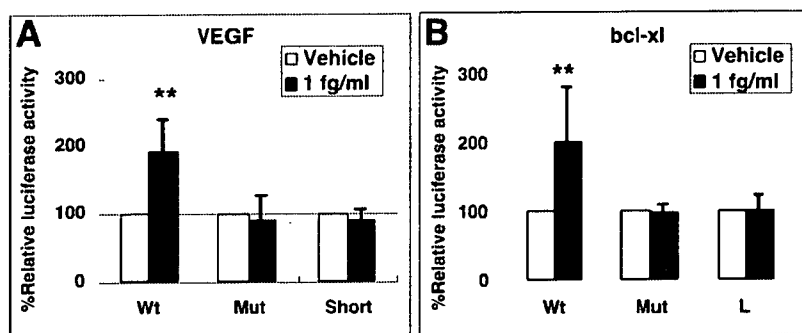


FIG. 11. Dihydrogensenoside Rb1 (dgRb1) transactivated VEGF and bcl-x promoter through HRE (hypoxia response element) and STRE (Stat5 response element), respectively. Cultured neurons were co-transfected with a renilla luciferase reporter vector (pRL-TK) and the following constructs. (A) VEGF promoter-luciferase plasmids carrying wild-type HRE (VEGF-wt), mutant HRE (VEGF-mut), and a plasmid that does not carry HRE (VEGF-short). (B) bcl-x-wt that carries STRE, bcl-x-mut in which the Stat response element has been mutated, and bcl-x-0.6L that does not carry STRE. After transfection, neurons were incubated for 24 h in the presence or absence of dgRb1 (1 fg/mL), and dual luciferase assay was carried out. Units of luciferase activity were normalized based on values of pRL-TK activity to control for transfection efficiency. Data were obtained from five independent experiments. Note that dgRb1 significantly increased relative luciferase activity of VEGF or bcl-x only when the VEGF-wt or bcl-x-wt plasmid was transfected in neurons, respectively. **Significantly higher ($p < 0.01$) than vehicle-treated control.

spinal tissue repair and nerve regeneration, and may ameliorate the cascade of progressive cell death.

In our previous study, we showed that gRb1 reorganized the cerebrovascular networks in the ischemic penumbra, suggesting that gRb1 could induce proliferation of endothelial cells and stimulate angiogenesis (Zhang et al., 2006). VEGF is considered to be the most endothelial cell-specific growth factor (Storkebaum et al., 2004) and gRb1 has been shown to increase VEGF expression in keratinocytes during wound-healing process (Kimura et al., 2006). Hence, we evaluated whether dgRb1 upregulated VEGF expression in neurons and showed that dgRb1 upregulated VEGF expression in neurons. VEGF was initially described in 1983 as a "tumor-secreted vascular permeability factor" (Senger et al., 1983) and was cloned in 1989 (Ferrara and Henzel, 1989). VEGF has been established to be an essential regulator of angiogenesis in a variety of human diseases (Ferrara et al., 2003). Although initial studies indicated that VEGF is an endothelial cell-specific factor, more recent findings revealed that VEGF also has direct effects on neural cells. In the dorsal root ganglia, VEGF stimulates axonal outgrowth and promotes the survival of neurons and satellite cells, whereas inhibition of VEGF receptor-2 (VEGFR-2) signaling blocks axonal outgrowth in response to VEGF (Sondell et al., 2000). VEGF also has neurotrophic effects on cultured neurons of the central nervous system and, in many instances, exerts this effect via signaling through VEGFR-2, phosphatidylinositol-3-kinase (PI3K) and Akt (Storkebaum et al., 2004). The ability of VEGF to stimulate angiogenesis and elicit di-

rect neurotrophic effects makes it an attractive candidate for repair or regeneration of the damaged brain tissue. In a model of cerebral ischemia, upregulation of VEGF was detected in the penumbra, where neovascularization and neuronal apoptosis of CNS are known to occur (Ferrer and Planas, 2003; Marti et al., 2000). However, VEGF up-regulation following brain damage may have deleterious effects due to its permeability-increasing activity *in vivo*. Following SCI, treatment with recombinant VEGF caused an improvement in recovery, associated with increased vessel density and reduced apoptosis in the lesion area, and increased expression of VEGFR1, VEGFR2, NP1, and NP2 (Widenfalk et al., 2003), while it was also found to have a worsening effect on lesions caused by SCI, possibly secondary to its effect on vascular permeability (Benton and Whittemore, 2003). The timing of VEGF treatment is probably an important determinant of its therapeutic effect on brain damage. Early treatment with VEGF (1 h post-ischemia) increased brain-blood barrier leakage, hemorrhagic transformation and ischemic lesions, while late treatment with VEGF (48 h post-ischemia) enhanced angiogenesis and significantly improved neurological recovery (Zhang et al., 2000). In this study, we showed that dgRb1-induced expression of VEGF resulted from transactivation of hypoxia-response-element, and an increase in the levels of VEGF mRNA and its translational product. We speculate that spontaneous late-onset upregulation of VEGF protein in neurons can ameliorate SCI and ischemic brain damage *in vivo*, and that the neuroprotective effects of VEGF result from a combination of the direct effects on

neuronal survival as well as the indirect consequences of increased angiogenesis. Further investigations are required to confirm these assumptions.

In this study, we also showed that dgRb1 upregulated Bcl-x_L expression in neurons, and dgRb1-induced expression of bcl-x_L mRNA was STRE dependent. Bcl-x_L, as a mitochondrion-associated protein, is widely expressed in the nervous system (Raghupathi, 2004; Sprick and Walczak, 2004). Mice deficient in Bcl-x_L die on embryonic day 13 (E13), and analysis of E12 mouse embryos shows massive death of immature postmitotic neurons throughout the brain and spinal cord as well as in the developing dorsal root ganglia (Motoyama et al., 1995). Moreover, overexpression of Bcl-x_L leads to increased survival of postnatal central neurons (Parsadanian et al., 1998). In the pathological mechanism of SCI and ischemic brain damage, insufficient expression of Bcl-x_L protein in response to SCI and brain damage appears to liberate Apat1 and cytochrome c, which form a complex with procaspase 9, leading to activation of procaspase 9 and caspase 9, and then to activation of the cell executioner, caspase 3 (Ouyang and Giffard, 2004). In fact, insulin-like growth factor 1 protected motor neurons through up-regulation of Bcl-x_L protein after SCI (Nakao et al., 2001). Administration of Bcl-x_L protein significantly increased neuronal survival after SCI (Nesic-Taylor et al., 2005) and after cerebral ischemia (Kilic et al., 2006). Consistent with these previous studies, our data suggested that administration of dgRb1 ameliorated SCI and ischemic brain damage, at least in part, through the upregulation of an anti-apoptotic factor, Bcl-x_L.

In addition, we showed that dgRb1 upregulated VEGF and Bcl-x_L expression via transactivation of HRE and STRE, respectively. HRE is an enhancer element of several hypoxia-regulated genes such as VEGF, erythropoietin (Epo), inducible form of nitric oxide synthase (iNOS) and glucose transporter 1 (Cummins and Taylor, 2005). The expression of these genes is of benefit in cell survival and recovery from ischemic insult. HRE, therefore, plays crucial roles in the oxygen-sensing mechanism. Furthermore, STRE has been identified as an Epo-responsive motif for the binding of a Stat 5 protein in the untranslated 5' region of the mouse bcl-x gene (Silva et al., 1999). Epo can function as a survival factor by repressing apoptosis through Bcl-x_L in erythroid progenitor cells, suggesting that STRE plays pivotal roles in the apoptotic cell death mechanism. At present, we have no evidence that dgRb1 can directly bind and transactivate both HRE and STRE. Since it is very rare that one molecule can bind two different response elements, we speculate that dgRb1 transactivates both HRE and STRE indirectly (for example, via activation of hypoxia-inducible fac-

tor-1 function and STAT5 function). Further investigations are required to confirm this assumption.

Finally, we showed that intravenous infusion of dgRb1 did not affect brain temperature, blood pressure or cerebral blood flow. These findings suggest that dgRb1 rescued damaged neurons without affecting systemic parameters. Since ginseng has been taken by many people in Asian countries for thousands of years without any detrimental effects, dgRb1 as a chemical derivative of gRb1 that is a main ginseng ingredient is expected to cause few adverse effects on humans. It is tempting to speculate that intravenous infusion of dgRb1 could be applied in patients with SCI or acute cerebral stroke without any adverse effects. DgRb1, that upregulates VEGF and Bcl-x_L at extremely low concentrations, may also be useful for the treatment of neurodegenerative diseases such as Parkinson disease and Alzheimer disease.

ACKNOWLEDGMENTS

We are grateful to Drs. T. Suzuki and Y. Ohta for providing stroke-prone spontaneously hypertensive rats and to Dr. K. Ikoma for his encouragement and valuable suggestions throughout this work. The technical assistance of Drs. F. Gu, K. Nakata and H. Fujita and the secretarial assistance of Ms. K. Hiraoka are acknowledged. This project was supported, in part, by grants from the Ministry of Education, Science, Sports and Culture of Japan.

REFERENCES

- BASSO, D.M., BEATTIE, M.S., and BRESNAHAN, J.C. (1995). A sensitive and reliable locomotor rating scale for open field testing in rats. *J. Neurotrauma* **12**, 1-21.
- BEATTIE, M.S. (2004). Inflammation and apoptosis: linked therapeutic targets in spinal cord injury. *Trends Mol. Med.* **10**, 580-583.
- BENTON, R.L., and WHITTEMORE, S.R. (2003). VEGF165 therapy exacerbates secondary damage following spinal cord injury. *Neurochem. Res.* **28**, 1693-1703.
- CUMMINS, E.P., and TAYLOR, C.T. (2005). Hypoxia-responsive transcription factors. *Pflugers Arch.* **450**, 363-371.
- ENOMOTO, M., WAKABAYASHI, Y., QI, M.L., and SHINOMIYA, K. (2004). Present situation and future aspects of spinal cord regeneration. *J. Orthop. Sci.* **9**, 108-112.
- FERRARA, N., GERBER, H.P., and LECOUTER, J. (2003). The biology of VEGF and its receptors. *Nat. Med.* **9**, 669-676.
- FERRARA, N., and HENZEL, W.J. (1989). Pituitary follicular cells secrete a novel heparin-binding growth factor specific for vascular endothelial cells. *Biochem. Biophys. Res. Commun.* **161**, 851-858.

NEUROPROTECTION BY DIHYDROGINSENOSE RB1

- FERRER, I., and PLANAS, A.M. (2003). Signaling of cell death and cell survival following focal cerebral ischemia: life and death struggle in the penumbra. *J. Neuropathol. Exp. Neurol.* **62**, 329–339.
- KILIC, E., KILIC, U., and HERMANN, D.M. (2006). TAT fusion proteins against ischemic stroke: current status and future perspectives. *Front. Biosci.* **11**, 1716–1721.
- KIMURA, Y., SUMIYOSHI, M., KAWAHIRA, K., and SAKANAKA, M. (2006). Effects of ginseng saponins isolated from Red Ginseng roots on burn wound healing in mice. *Br. J. Pharmacol.* **148**, 860–870.
- LAEMMLI, U.K. (1970). Cleavage of structural proteins during the assembly of the head of bacteriophage T4. *Nature* **227**, 680–685.
- MARTI, H.J., BERNAUDIN, M., BELLAIL, A., et al. (2000). Hypoxia-induced vascular endothelial growth factor expression precedes neovascularization after cerebral ischemia. *Am. J. Pathol.* **156**, 965–976.
- MORINO, T., OGATA, T., HORIUCHI, H., et al. (2003). Delayed neuronal damage related to microglia proliferation after mild spinal cord compression injury. *Neurosci. Res.* **46**, 309–318.
- MOTOYAMA, N., WANG, F., ROTH, K.A., et al. (1995). Massive cell death of immature hematopoietic cells and neurons in Bcl-x-deficient mice. *Science* **267**, 1506–1510.
- NAKAO, Y., OTANI, H., YAMAMURA, T., HATTORI, R., OSAKO, M., and IMAMURA, H. (2001). Insulin-like growth factor I prevents neuronal cell death and paraplegia in the rabbit model of spinal cord ischemia. *J. Thorac. Cardiovasc. Surg.* **122**, 136–143.
- NARUO, S., OKAJIMA, K., TAOKA, Y., et al. (2003). Prostaglandin E1 reduces compression trauma-induced spinal cord injury in rats mainly by inhibiting neutrophil activation. *J. Neurotrauma* **20**, 221–228.
- NESIC-TAYLOR, O., CITTELLY, D., YE, Z., et al. (2005). Exogenous Bcl-xL fusion protein spares neurons after spinal cord injury. *J. Neurosci. Res.* **79**, 628–637.
- OUYANG, Y.B., and GIFFARD, R.G. (2004). Cellular neuroprotective mechanisms in cerebral ischemia: Bcl-2 family proteins and protection of mitochondrial function. *Cell Calcium* **36**, 303–311.
- PARSADANIAN, A.S., CHENG, Y., KELLER-PECK, C.R., HOLTZMAN, D.M., and SNIDER, W.D. (1998). Bcl-xL is an antiapoptotic regulator for postnatal CNS neurons. *J. Neurosci.* **18**, 1009–1019.
- PROFYRIS, C., CHEEMA, S.S., ZANG, D., AZARI, M.F., BOYLE, K., and PETRATOS, S. (2004). Degenerative and regenerative mechanisms governing spinal cord injury. *Neurobiol. Dis.* **15**, 415–436.
- RAGHUPATHI, R. (2004). Cell death mechanisms following traumatic brain injury. *Brain Pathol.* **14**, 215–222.
- SAMUKAWA, H., YAMASHITA, H., MATSUDA, H., and KUBO, M. (1995). Simultaneous analysis of saponins in Ginseng Radix by high performance liquid chromatography. *Chem. Pharm. Bull.* **43**, 137–141.
- SAYER, F.T., KRONVALL, E., and NILSSON, O.G. (2006). Methylprednisolone treatment in acute spinal cord injury: the myth challenged through a structured analysis of published literature. *Spine J.* **6**, 335–343.
- SENGER, D.R., GALLI, S.J., DVORAK, A.M., PERRUZZI, C.A., HARVEY, V.S., and DVORAK, H.F. (1983). Tumor cells secrete a vascular permeability factor that promotes accumulation of ascites fluid. *Science* **219**, 983–985.
- SHIBATA, S., TANAKA, O., SHOJI, J., and SAITO, H. (1994). Chemistry and pharmacology of Panax, in: *Economic and Medicinal Plant Research* H. Wagner, H. Hikino, and R.N. Earnsworth (eds), World Scientific: Philadelphia, pps. 217–284.
- SILVA, M., BENITO, A., SANZ C., et al. (1999). Erythropoietin can induce the expression of bcl-x(L) through Stat5 in erythropoietin-dependent progenitor cell lines. *J. Biol. Chem.* **274**, 22165–22169.
- SONDELL, M., SUNDLER, F., and KANJE, M. (2000). Vascular endothelial growth factor is a neurotrophic factor which stimulates axonal outgrowth through the flk-1 receptor. *Eur. J. Neurosci.* **12**, 4243–4254.
- SPRICK, M.R., and WALCZAK, H. (2004). The interplay between the Bcl-2 family and death receptor-mediated apoptosis. *Biochim. Biophys. Acta.* **1644**, 125–132.
- STORKEBAUM, E., LAMBRECHTS, D., and CARMELIET, P. (2004). VEGF: once regarded as a specific angiogenic factor, now implicated in neuroprotection. *Bioessays* **26**, 943–954.
- SWANSON, R.A., MORTON, M.T., TSAO, W.G., SAVALOS, R.A., DAVIDSON, C., and SHARP, F.R. (1990). A semiautomated method for measuring brain infarct volume. *J. Cereb. Blood Flow Metab.* **10**, 290–293.
- TOKU, K., TANAKA, J., YANO, H., et al. (1998). Microglial cells prevent nitric oxide-induced neuronal apoptosis in vitro. *J. Neurosci. Res.* **53**, 415–425.
- WIDENFALK, J., LIPSON, A., JUBRAN, M., et al. (2003). Vascular endothelial growth factor improves functional outcome and decreases secondary degeneration in experimental spinal cord contusion injury. *Neuroscience* **120**, 951–960.
- ZHANG, B., HATA, R., ZHU, P., et al. (2006). Prevention of ischemic neuronal death by intravenous infusion of a ginseng saponin, ginsenoside Rb(1), that upregulates Bcl-x(L) expression. *J. Cereb. Blood Flow Metab.* **26**, 708–721.
- ZHANG, B., TANAKA, J., YANG, L., et al. (2004). Protective effect of vitamin E against focal brain ischemia and neuronal death through induction of target genes of hypoxia-inducible factor-1. *Neuroscience* **126**, 433–440.

SAKANAKA ET AL.

ZHANG, Z., and GUTH, L. (1997). Experimental spinal cord injury: Wallerian degeneration in the dorsal column is followed by revascularization, glial proliferation, and nerve regeneration. *Exp. Neurol.* **147**, 159-171.

ZHANG, Z.G., ZHANG, L., JIANG, Q., et al. (2000). VEGF enhances angiogenesis and promotes blood-brain barrier leakage in the ischemic brain. *J. Clin. Invest.* **106**, 829-838.

Address reprint requests to:

Ryuji Hata, M.D., Ph.D.

Department of Functional Histology

Ehime University Graduate School of Medicine

Shitakawa, Toon

Ehime 791-0295, Japan

E-mail: hata@m.chime-u.ac.jp

HEMATOPOIETIC STEM CELLS PREVENT HAIR CELL DEATH AFTER TRANSIENT COCHLEAR ISCHEMIA THROUGH PARACRINE EFFECTS

T. YOSHIDA,^a N. HAKUBA,^a I. MORIZANE,^a K. FUJITA,^a
F. CAO,^b P. ZHU,^b N. UCHIDA,^c K. KAMEDA,^d
M. SAKANAKA,^b K. GYO^a AND R. HATA^{a,b*}

^aDepartment of Otolaryngology, Ehime University Graduate School of Medicine, Shitsukawa, Toon, Ehime 791-0295, Japan

^bDepartment of Functional Histology, Ehime University Graduate School of Medicine, Shitsukawa, Toon, Ehime 791-0295, Japan

^cDepartment of Internal Medicine 1, Ehime University Graduate School of Medicine, Shitsukawa, Toon, Ehime 791-0295, Japan

^dIntegrated Center for Science, Ehime University Graduate School of Medicine, Shitsukawa, Toon, Ehime 791-0295, Japan

Abstract—Transplantation of hematopoietic stem cells (HSCs) is regarded to be a potential approach for promoting repair of damaged organs. Here, we investigated the influence of hematopoietic stem cells on progressive hair cell degeneration after transient cochlear ischemia in gerbils. Transient cochlear ischemia was produced by extracranial occlusion of the bilateral vertebral arteries just before their entry into the transverse foramen of the cervical vertebra. Intrascalar injection of HSCs prevented ischemia-induced hair cell degeneration and ameliorated hearing impairment. We also showed that the protein level of glial cell line-derived neurotrophic factor (GDNF) in the organ of Corti was upregulated after cochlear ischemia and that treatment with HSCs augmented this ischemia-induced upregulation of GDNF. A tracking study revealed that HSCs injected into the cochlea were retained in the perilymphatic space of the cochlea, although they neither transdifferentiated into cochlear cell types nor fused with the injured hair cells after ischemia, suggesting that HSCs had therapeutic potential possibly through paracrine effects. Thus, we propose HSCs as a potential new therapeutic strategy for hearing loss. © 2007 IBRO. Published by Elsevier Ltd. All rights reserved.

Key words: cochlear ischemia, hematopoietic stem cell, stem cell therapy, hearing loss, hair cell death, GDNF.

The prevalence of acquired hearing loss is very high. About 10% of the total population and more than one third of the population over 65 years suffer from debilitating hearing loss (Li et al., 2004). The most common type of hearing loss in adults is sensorineural hearing loss (SNHL). In the majority of cases, SNHL is permanent and

typically associated with loss of sensory hair cells in the organ of Corti. Humans are born with a complement of about 16,000 sensory hair cells and 30,000 auditory neurons in each ear. Sensory hair cells and auditory neurons do not regenerate throughout life, and loss of these cells is irreversible and cumulative. At present, the only therapeutic intervention for patients with profound SNHL is a cochlear implant that electrically stimulates residual primary auditory neurons. In many cases, a cochlear prosthesis and associated speech processor can restore accurate speech reception to a person who otherwise has little or no auditory sensitivity. For the last two decades, cochlear implants have been in common clinical use. Following the loss of sensory hair cells, however, the auditory neurons undergo secondary degeneration. Evidence from animal studies indicates that ongoing degeneration of auditory neurons has the potential to compromise the efficacy of a cochlear implant (Shepherd et al., 2004). From the clinical perspective, there are likely to be benefits if sensory hair cells can be rescued.

Recent advances in stem cell biology have provided hope that stem cell therapy will come closer to regenerating sensory hair cells in humans. A major advance in the prospects for the use of stem cells to restore normal hearing comes with the recent discovery that hair cells can be generated *ex vivo* from embryonic stem (ES) cells, adult inner ear stem cells and neural stem cells (Li et al., 2003a,b; Tateya et al., 2003). These stem cells are pluripotent, such that all cell types in the inner ear can be derived from them. Furthermore, stem cells can secrete several kinds of trophic factors. There is increasing evidence that stem cells can promote host neural repair in part by secreting diffusible molecules such as growth factors (Mahmood et al., 2004). These findings suggest that stem-cell-based treatment regimens could be applicable to the damaged inner ear as future clinical applications. Previously we have shown that neural stem cells can prevent ischemia-induced inner hair cell (IHC) loss and ameliorate hearing impairment. Among the several types of stem cells, we propose that hematopoietic stem cells (HSCs) are one of the best candidates for stem cell therapy in clinical practice, because autologous transplantation can not only eliminate the need to find suitable donors, but can also avoid the problems of immunological incompatibility and ethical concerns. In this study, we explored the feasibility of HSC transplantation as therapy for hearing loss.

EXPERIMENTAL PROCEDURES

All experiments were conducted according to the U.S. National Institutes of Health Guide for the Care and Use of Laboratory

*Corresponding author. Tel: +81-89-960-5236; fax: +81-89-960-5239.

E-mail address: hata@m.ehime-u.ac.jp (R. Hata).

Abbreviations: ABR, auditory brainstem response; Ang1, angiopoietin-1; BDNF, brain-derived neurotrophic factor; DMEM, Dulbecco's modified Eagle's medium; EPO, erythropoietin; FCS, fetal calf serum; FGF, fibroblast growth factor; GDNF, glial cell line-derived neurotrophic factor; HSC, hematopoietic stem cell; IHC, inner hair cell; OHC, outer hair cell; PI, propidium iodide; SDS, sodium dodecylsulfate; SNHL, sensorineural hearing loss; SP, side population.

0306-4522/07\$30.00+0.00 © 2007 IBRO. Published by Elsevier Ltd. All rights reserved.
doi:10.1016/j.neuroscience.2006.12.067

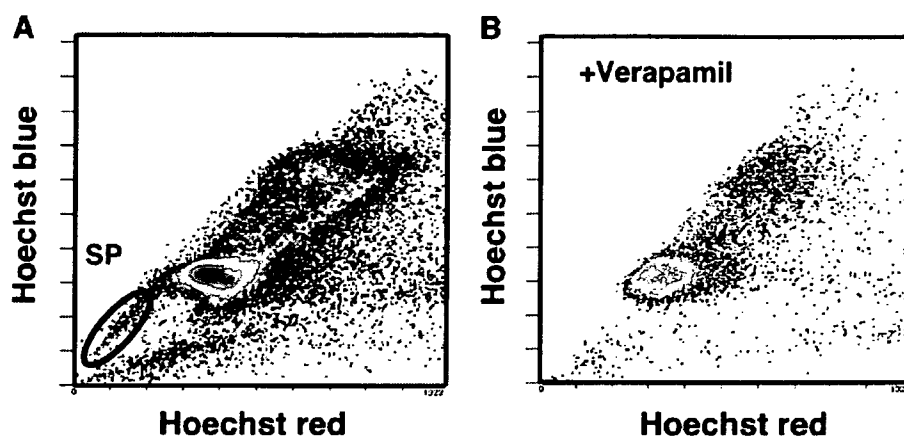


Fig. 1. Flow cytometric analysis of SP cells in Hoechst-stained bone marrow (BM). SP region of whole BM stained with Hoechst in the absence (A) and presence (B) of 50 μM verapamil. The region marked SP was sorted for transplantation experiments. Approximately 0.2–0.4% of cells fell into the SP gate.

Animals (NIH Publication No. 80-23) and were approved by the Ethics Committee at Ehime University Graduate School of Medicine. All efforts were made to minimize the number of animals used and their suffering. Animals were housed in an animal room with a temperature of 21–23 °C and a 12-h light/dark cycle (light on: 7 a.m. to 7 p.m.). Animals were allowed access to food and water *ad libitum* until the end of the experiment.

Induction of transient cochlear ischemia

Adult male Mongolian gerbils weighing 60–80 g were used in this study. Following the methods of Hata et al. (1993), transient cochlear ischemia was induced by temporarily occluding bilateral vertebral arteries in the neck, since they lack the posterior cerebral communicating arteries and the labyrinthine arteries are nourished solely by the vertebro-basilar system. Anesthesia was induced with 3% halothane in a 7:3 mixture of nitrous oxide and oxygen, and maintained with 1% halothane. An anterior midline cervical incision was made, and bilateral vertebral arteries were exposed just before their entry into the transverse foramen of the cervical vertebra. Then, a 4–0 silk suture was loosely looped around each vertebral artery. The animals were orotracheally intubated, and artificially ventilated to prevent systemic anoxia. The tidal volume was set at 1 ml and the ventilation rate at 70/min. Ischemia was induced in both cochleae by pulling the ligatures with 5 g weights. After 15 min of ischemia, the sutures were removed to allow recirculation, which was confirmed by observation with an operating microscope. Some gerbils were sham-operated as control animals, where bilateral vertebral arteries were exposed but no arterial occlusion took place. Rectal temperature was maintained at 37 °C with a heat lamp during the surgical procedure.

Isolation of HSCs

Bone marrow specimens were extracted from the tibiae and femurs of 6–12-week-old gerbils. The bone marrow cells were suspended at 10^6 cells/ml in pre-warmed Dulbecco's modified Eagle's medium (DMEM) containing 2% fetal calf serum (FCS). HSCs were isolated by the method described by Goodell et al. (1996). In brief, the bone marrow cells were stained with 5 $\mu\text{g}/\text{ml}$ Hoechst 33342 (Sigma Chemical Co., St. Louis, MO, USA) for 90 min at 37 °C. Analysis and sorting were executed with an EPICS ALTRA flow cytometer (Beckman Coulter, Inc., Fullerton, CA, USA). Hoechst dye was excited with a UV laser at 333.4–363.8 nm. Two wavelengths, obtained by using a 450 BP

filter (Hoechst Blue) and a 675 EFLP optical filter (Hoechst Red), were used to measure its fluorescence. Propidium iodide (PI) fluorescence was also measured at 675 EFLP (having been excited at 350 nm). Cells stained with PI were seen on the far right of Hoechst red (675 EFLP) and excluded. The addition of PI allowed exclusion of dead cells and did not affect the Hoechst staining profile. Both Hoechst blue and red fluorescence are shown on a linear scale. The gating on forward and side scatter was not rigorous, and excluded only erythrocytes and debris. The side population (SP) sorting gates were defined on the flow cytometer using Hoechst red and blue axes to exclude dead cells, erythrocytes (no Hoechst stain), and debris. After collecting 10^5 events within this live gate, the SP population could be clearly identified and defined and was considered as HSCs (Goodell et al., 1996). The gate established on this population is shown in Fig. 1A.

Administration of HSCs

One day before the induction of transient cochlear ischemia, the gerbils received HSCs (2×10^3 cells/ μl in DMEM, total 4 μl) in their left cochleae. The right cochlea of each animal was treated with vehicle (DMEM; total 4 μl) and used as vehicle control. Under halothane anesthesia, the otic bulla was opened through a retroauricular approach and the round window was exposed. A 0.15-mm-diameter glass microtube was inserted into the scala tympani through the round window with a micromanipulator. HSCs or vehicle were infused at a flow rate of 1 $\mu\text{l}/\text{min}$ for 4 min using a microinfusion pump.

Recording of auditory brainstem response (ABR)

Hearing of the animal was assessed before and 4 days after ischemic insult by sequential recording of ABR. Under halothane anesthesia, ABR was recorded using a signal processor (NEC Synax 1200, NEC Medical Systems, Tokyo, Japan). Stimulus sound was led to the ear canal via a tiny polypropylene tube; thus each ear was stimulated separately. Recording needle electrode was placed at the vertex and retroauricle. As the animal did not tolerate long-term anesthesia, ABR was recorded only to 8000-Hz tone burst (0.5 ms rise/fall time and 10 ms duration). Cochlear region corresponding to the tone of this frequency was proved most vulnerable to ischemic injury, according to our previous study (Hakuba et al., 2003b). Responses to 300 consecutive stimuli were averaged, and the threshold of ABR was determined by measuring the responses in 5 dB steps.

Evaluation of hair cell loss

The degree of hair cell loss was assessed by staining the cochlea with rhodamine-phalloidin and Hoechst 33342. Rhodamine-phalloidin is appropriate for observation of cell architecture and Hoechst 33342 for their nuclei. Four days after ischemia, the organs of Corti were dissected out by means of a surface preparation and were stained with rhodamine-phalloidin (Hakuba et al., 2003b). Fluorescence was detected using an Olympus BX60 microscope (Olympus, Tokyo, Japan) with a green filter and a UV filter. The numbers of intact and dead hair cells were counted in the basal turn of the cochlea, and the ratio of intact to dead hair cells was calculated.

Western blot analysis

After deep anesthesia with an i.p. injection of sodium pentobarbital (0.1 g/kg), the otic bulla (wet weight 10 mg) was removed and transferred to ice-cold PBS. The samples were homogenized in microcentrifuge tubes containing 100 μ l lysis buffer (0.5% sodium dodecylsulfate (SDS), 0.5% Triton-X, 100 μ M phenylmethane sulfonyl fluoride, 20 μ M Tris-HCl pH 8.0). The homogenates were sonicated on ice and centrifuged at 13,000 r.p.m. for 10 min at 4 °C. The protein content in the supernatant was determined using a BCA protein assay kit (Pierce, Rockland, IL, USA) with bovine serum albumin as a standard. The supernatant was mixed with sample buffer (62.5 mM Tris-HCl, pH 6.8, 2% SDS, 10% glycerol and 0.001% Bromophenol Blue) to a final protein concentration of 1 mg/ml. The samples were boiled for 5 min. Equal amounts of protein (15 μ g/lane) were resolved by SDS-PAGE electrophoresis, transferred onto a nitrocellulose membrane, and immunoblotted with an antibody against glial cell line-derived neurotrophic factor (GDNF) (sc-328, Santa Cruz Biotechnology, Santa Cruz, CA, USA). Densitometric analysis of scanned bands was performed to quantify the GDNF protein levels in the samples. The integrated optical density was obtained using a NIH Image program (National Institutes of Health, Bethesda, MD, USA). The data were normalized to internal standards (vehicle-treated control) on each gel and expressed in percentage.

PKH67 staining

The sorted cells were labeled using a fluorescent membrane dye, PKH67 (Sigma), which excites at a wavelength of 496 nm and emits at 520 nm. According to the manufacturer's instructions, samples were stained with PKH67 at room temperature for 10 min. Staining was stopped by addition of four volumes of DMEM containing 10% FCS. The cells were collected by centrifugation (1500 r.p.m., 10 min, 4 °C), and washed twice with DMEM.

Tissue preparation for short-term cellular tracking

The gerbils were treated with PKH-labeled HSCs as described above. Four days after ischemic insult, they were deeply anesthetized intraperitoneally with a lethal dose of sodium pentobarbital (0.5 g/kg), and perfused intracardially with saline, followed by 4% paraformaldehyde in PBS. The temporal bones were removed and fixed in the same fixative at 4 °C for 4 h. In some animals, the fixed temporal bones were decalcified with 0.1 M EDTA for 24 h at 4 °C and 10- μ m-thick cryostat sections of the temporal bone were prepared. The sections were then mounted on 3-aminopropyl triethoxysaline (APS)-coated slide glasses. In other animals, the organs of Corti in the fixed temporal bones were dissected out by means of a surface preparation, stained with rhodamine-phalloidin and mounted on slide glasses as described above. The sections were viewed with an Olympus BX60 fluorescence microscope.

Statistical analysis

All values are presented as mean \pm S.D. The changes in ABR threshold between the vehicle-treated side and HSC-treated side were analyzed using two-tailed Mann-Whitney *U* test. All other statistical significances were tested by one way ANOVA followed by Bonferroni's multiple comparison test. A *P* value less than 0.05 was considered statistically significant.

RESULTS

ABR threshold shift

We initially evaluated the sequential changes in hearing by ABR in six gerbils. ABR threshold to 8000 Hz tone burst was approximately 30 dB SPL in normal animals, which was significantly elevated by ischemic insult. Hearing deterioration was prevented by pre-ischemic transplantation of HSCs (Fig. 2). Four days after ischemia, the average increase in the ABR threshold on the vehicle-treated side was 32.5 ± 7.6 [mean \pm S.D.] dB. In contrast, the average increase in ABR threshold on the HSC-treated side was 16.9 ± 5.9 dB. These results suggested that treatment with HSCs ameliorated the ischemia-induced hearing impairment.

Morphological study

Previously, we reported that cochlear ischemia for 15 min resulted in progressive IHC loss by 4 days after ischemia, while a little outer hair cell (OHC) loss was observed (Watanabe et al., 2001). We also reported that this progressive IHC loss was closely related to hearing impairment evaluated by ABR (Watanabe et al., 2001). Hence, we next investigated the effects of HSC transplantation on ischemia-induced IHC loss. Hair cell loss was identified at

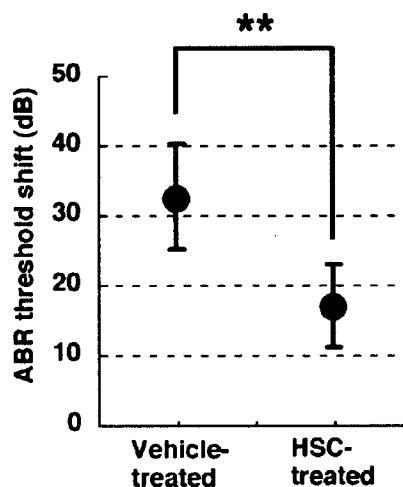


Fig. 2. ABR threshold at 4 days after cochlear ischemia. Pretreatment with HSCs (HSC-treated) significantly suppressed the elevation of threshold in comparison with the vehicle-treated control. The average ABR threshold shift on the vehicle- and HSC-treated sides ($n=6$ in each side) was analyzed using two-tailed Mann-Whitney *U* test. A *P* value less than 0.05 was considered statistically significant. Double asterisk indicates statistical significance ($P < 0.01$). All values are presented as mean \pm S.D.

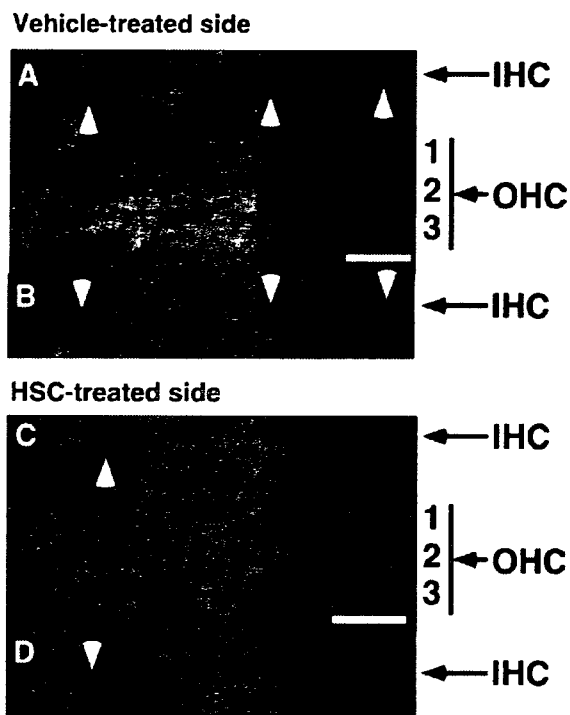


Fig. 3. Surface structure of organ of Corti at 4 days after cochlear ischemia. Representative fluorescence images of the organ of Corti stained with rhodamine-phalloidin (A and C) and Hoechst 33342 (B and D). Gerbils were subjected to cochlear ischemia for 4 days. The organs of Corti were obtained from the otic bullae on the vehicle-treated side (A and B) and HSC-treated side (C and D). There are three rows of OHCs and a single row of IHCs. Fluorescence microscopy revealed fewer deficits in IHCs on the HSC-treated side than on the vehicle-treated side. Scale bar=20 μ m. Arrowheads indicate deficits in IHCs.

4 days after ischemia while only a small hair cell loss was identified in normal animals (Fig. 3). It is apparent that the stereocilia of hair cells on the vehicle-control side disappeared sporadically. In contrast, the hair cell loss was ameliorated in the specimen obtained from the HSC-treated side. The percentages of hair cell loss are summarized in Fig. 4. In each group ($n=6$), cell loss was more prominent in IHCs than in OHCs. In IHCs, the percentage of cell loss was $23.6 \pm 4.0\%$ on the vehicle-treated side and $8.2 \pm 4.0\%$ on the HSC-treated side. The difference was statistically significant ($P < 0.01$). In OHCs, the percentage of cell loss was $2.5 \pm 1.4\%$ on the vehicle-treated side and $2.9 \pm 2.4\%$ on the HSC-treated side, representing no significant difference. These results were consistent with a greater change of ABR threshold in the vehicle-treated control, compared with that in the HSC-treated group.

Fate of HSCs injected into organ of Corti

We next investigated whether the HSCs transdifferentiated into cochlear cell types or fused with the injured hair cells after cochlear ischemia. To confirm the fate of HSCs, we used PKH67 for short-term tracking *in vivo*. PKH has been used for cellular tracking (Punzel et al., 2001), and this dye has been demonstrated to be stable on the surface of

quiescent cells for periods exceeding 3 weeks, does not compromise cellular viability, and does not impair the capacity of stem cells to reconstitute hematopoiesis in myeloablated recipients (Askenasy and Farkas, 2002). By using this dye (Fig. 5A and B), tracking of the HSCs injected into the cochleae was performed at 4 days after ischemia. In a 10- μ m-thick cryostat section, transplanted cells were predominantly located in the perilymphatic space of the cochlea (Fig. 5C and D). In sections of a cochlear surface preparation that were washed with PBS several times, no PKH-labeled cells were observed in hair cells and supporting cells of the organ of Corti (Fig. 5E and F). These results suggested that transplanted HSCs were retained within the perilymphatic space of the cochlea, but neither transdifferentiated into cochlear cells nor fused with the injured hair cells.

Induction of trophic factor after cochlear ischemia

To gain an insight into the mechanisms underlying IHC survival, we investigated the changes in the expression of GDNF, brain-derived neurotrophic factor (BDNF), fibroblast growth factor (FGF)1, FGF2, angiopoietin-1 (Ang1), neurotrophin-3 (NT3) and erythropoietin (EPO). Among them, only GDNF protein expression was markedly up-regulated by treatment with HSCs after cochlear ischemia. As shown in Fig. 6A, a single protein band of the expected size (approximately 35 kDa) for GDNF was detected by Western blot with a GDNF-specific primary antibody. No band was detected when the blots were incubated without primary antibody (data not shown). Five independent experiments were carried out and the results of densitometric

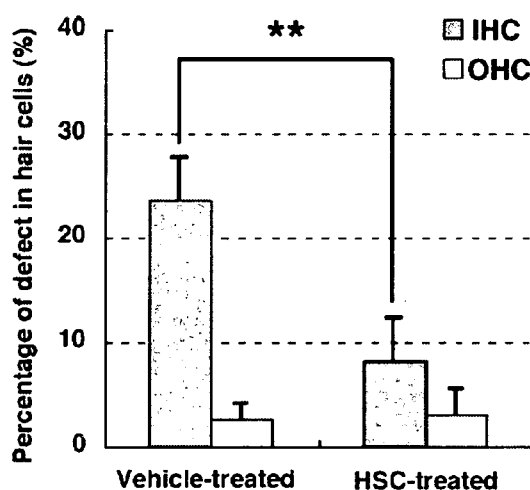


Fig. 4. Percentages of defects in IHCs and OHCs at 4 days after cochlear ischemia. Pretreatment with HSCs significantly reduced IHC damage at 4 days after cochlear ischemia. On the HSC-treated side ($n=6$), the proportion of deficits in IHCs was lower than that on the vehicle-treated side ($n=6$). On the other hand, there was no statistically significant difference in the amount of OHC loss between the HSC-treated side and vehicle-treated side. Statistical analysis was performed by one-way ANOVA followed by Bonferroni's multiple comparison test. A P value less than 0.05 was considered statistically significant. Double asterisk indicates statistical significance ($P < 0.01$). All values are presented as mean \pm S.D.

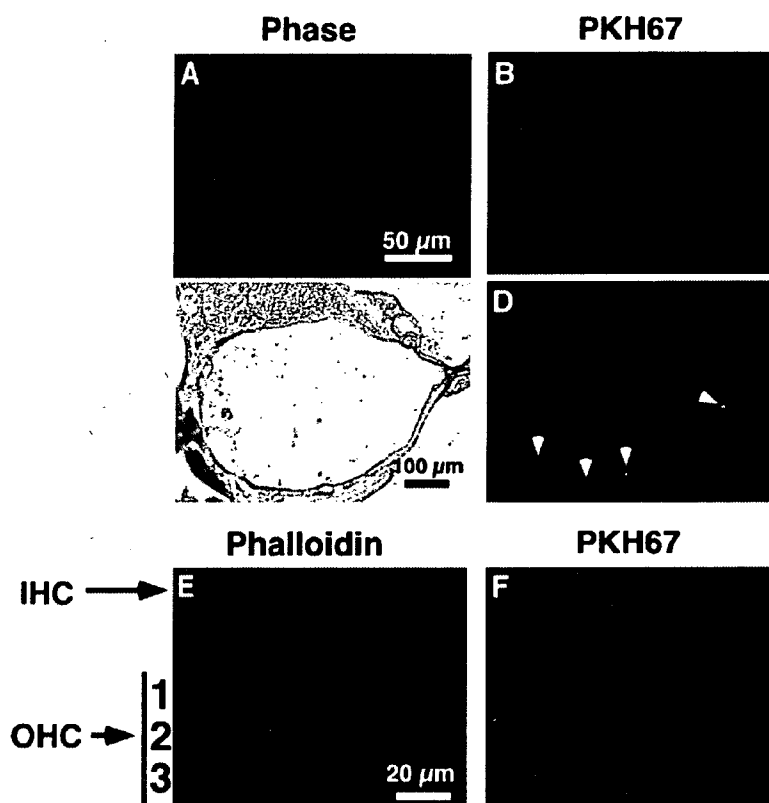


Fig. 5. PKH67 labeling. HSCs were labeled with PKH67 (B: green). Gerbils were treated with PKH67-labeled HSCs. One day later, animals were subjected to cochlear ischemia for 15 min. Four days after ischemia, the temporal bones were dissected out, fixed, decalcified and cut into 10- μ m-thick cryostat sections at -20°C . PKH67-positive cells were located in the perilymphatic space of the cochlea (D: green, arrowheads). In addition, other animals were treated with PKH67-labeled HSCs, and the temporal bones were dissected out and fixed. Then, the organs of Corti were dissected out by means of a surface preparation and visualized with rhodamine-phalloidin (E: red). No PKH-labeled cells were observed in hair cells, supporting cells, and other types of cochlear cells throughout the organ of Corti (F). Scale bars=50 μ m (A and B), 100 μ m (C and D), 20 μ m (E and F).

analysis are shown in Fig. 6B. In sham-operated animals, there was no significant difference in the level of GDNF protein between the vehicle-treated control and HSC-treated group. In contrast, the level of GDNF protein was significantly increased at 4 days after cochlear ischemia. The increase of the GDNF protein level was more prominent in the HSC-treated group than in the vehicle-treated control. These results revealed that ischemia-induced GDNF expression was augmented by treatment with HSCs.

DISCUSSION

In the present study, we used an animal model of transient cochlear ischemia induced by extracranial occlusion of the bilateral vertebral arteries in gerbils. This animal model has been described as a brain stem ischemia model. By using this animal model, selective vulnerability to ischemia in the brain stem was closely observed (Hata et al., 1993). This brainstem ischemia model has the following advantages: (1) it avoids intracranial injury, (2) it produces severe reproducible brainstem ischemia, and (3) it allows reperfusion. We also showed that reversibility of the ABR after reperfusion was correlated with ischemic lesions in the acoustic relay nuclei in the brainstem (Hata et al., 1998).

Because the inner ear is supplied by the labyrinthine artery from the basilar artery, Hakuba et al. (1997) first introduced this animal model as a cochlear ischemia model, and showed progressive IHC loss up to 4 days after cochlear ischemia (Hakuba et al., 2000; Watanabe et al., 2001). Our series of studies showed that this progressive IHC degeneration was induced by the ischemia-induced increase of glutamate concentration in the perilymph, activation of AMPA/kainate receptors on the presynaptic membrane of IHCs, and the subsequent accumulation of intracellular Ca^{2+} in IHCs, leading to cell death (Hakuba et al., 2003a; Hyodo et al., 2001; Maetani et al., 2003; Morizane et al., 2005; Taniguchi et al., 2002). Impairment of cochlear blood flow is thought to play an important role in the etiology of sudden deafness, presbycusis and noise-induced hearing loss (Nakashima et al., 2003; Seidman et al., 1999). Because of the fact that 90–95% of afferent sensory neurons synapse on IHCs and only 5% of neurons synapse on OHCs (Spoendlin, 1967), IHCs are thought to be the main mechanosensory cells that transform mechanical stimuli into neuronal signals (Brandt et al., 2003). In this ischemia model, the mean inter-peaked latency between waves I and V of ABR was not changed (K. Fujita, unpublished

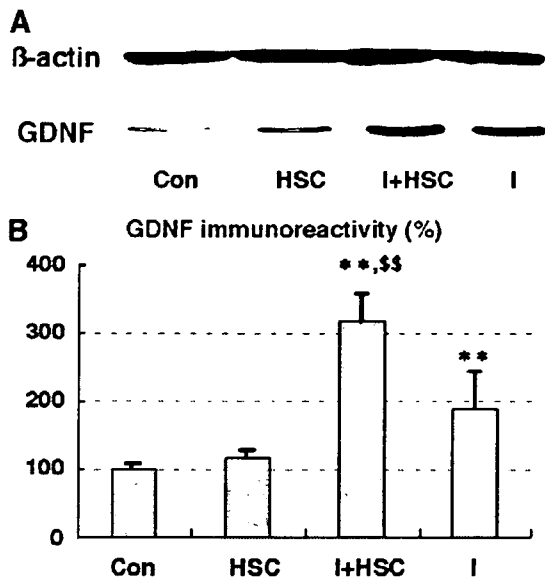


Fig. 6. Western blot analyses of GDNF in gerbil cochlea on the vehicle-treated and HSC-treated side. Samples were derived from the cochlear on the vehicle-treated side (Con) and HSC-treated side (HSC) in sham-operated gerbils, and on the vehicle-treated side (I) and HSC-treated side (I+HSC) in gerbils subjected to cochlear ischemia. Statistical analysis was performed by one-way ANOVA followed by Bonferroni's multiple comparison test. A P value less than 0.05 was considered statistically significant. ** Indicates significantly greater than vehicle-treated control (Con) ($P < 0.01$). \$\$ Indicates significantly greater than vehicle-treated group with cochlear ischemia (I) ($P < 0.01$). Data were obtained from five independent experiments. All values are presented as mean \pm S.D.

observations), suggesting that main ischemic lesion was not located within the brain stem. Furthermore, IHC loss started 1 day after ischemia and peaked at 4 days after ischemia, whereas neuronal loss in the spiral ganglion started at 4 days after ischemia and peaked at 7 days after ischemia. These data suggested that ischemia-induced IHC loss resulted in the secondary degeneration of the spiral ganglion neurons (K. Fujita, unpublished observations). In fact we showed that progressive IHC loss was closely related to hearing impairment evaluated by ABR (Watanabe et al., 2001). In the present study, we clearly showed that treatment with HSCs ameliorated this progressive IHC damage and prevented a shift in the ABR threshold after transient cochlear ischemia in gerbils.

The precise mechanism by which intrascalar injection of HSCs prevented ischemia-induced progressive IHC damage is unclear. There are several possibilities to enable functional recovery by treatment with HSCs. One explanation is that HSCs can induce the endogenous cochlear cells to proliferate and differentiate into hair cells to rescue or restore hearing loss. Several studies have shown that both neural stem cells and inner ear stem cells have the ability to differentiate into different inner ear cell types *in vivo* (Tateya et al., 2003) or *in vitro* (Li et al., 2003b). Recent studies have shown that HSCs are capable of transdifferentiating into a variety of nonhematopoietic lineages in multiple organs (Masson et al., 2004).

Another explanation is that HSCs can fuse with damaged hair cells and restore their function. A Cre/lox recombination system to identify transplanted cells indicated that bone marrow-derived stem cells fused with hepatocytes in the liver, with Purkinje neurons in the brain, and with cardiac muscle in the heart, resulting in the formation of multinucleated cells (Alvarez-Dolado et al., 2003). After transplantation of bone marrow from female wild-type mice into male fumarylacetoacetate hydrolase knockout mice, analysis of DNA from the tertiary recipients revealed that hepatocytes derived from bone marrow arose from cell fusion and not by transdifferentiation of HSCs (Wang et al., 2003). These reports suggested that cell fusion is responsible for phenotypic changes of HSCs into the target cells. The third explanation is that HSCs can promote hair cell repair in part by secreting trophic factors. It has been reported that production of trophic factors from stem cells can confer resistance to disease, or promote the survival, migration, and differentiation of endogenous precursors (Chopp and Li, 2002). Stem cell transplantation may be linked to the up-regulation of trophic factors (Mahmood et al., 2004). These reports suggest the possibility that stem cells can also play a part in promoting functional recovery by means other than cell replacement. In fact, bone marrow stem cells and neural stem cells are also known to secrete interleukins and neurotrophic factors (NGF, BDNF, and GDNF) (Crigler et al., 2006; Mahmood et al., 2004). Furthermore, HSCs were reported to secrete growth factors with neurotrophic properties, such as Ang1 (Takakura et al., 2000). In the present study, no PKH-labeled HSCs were observed throughout the organ of Corti. PKH-labeled HSCs were predominantly located in the perilymphatic space of the cochlea. These findings revealed that HSCs could survive in the perilymphatic space in the cochlea, and that at least in our experimental conditions, HSCs were not incorporated into hair cells, supporting cells, and other types of cells in the organ of Corti through cell fusion or transdifferentiation. For these reasons, the third explanation may be preferable, although further cellular and molecular biological investigations are required to clarify its mechanism.

It is well known that several kind of trophic factors including GDNF play a crucial role in the survival of sensory hair cells and auditory neurons (Gillespie and Shepherd, 2005; Roehm and Hansen, 2005). Because the protection by HSCs against ischemia-induced hair cell damage appeared to occur through their paracrine effects, we evaluated the ischemia-induced alterations of trophic factors (i.e. FGF1, FGF2, BDNF, NT-3, EPO, Ang1 and GDNF) in the cochlea. Consequently, we revealed that only GDNF expression was up-regulated after cochlear ischemia, and this ischemia-induced GDNF expression was augmented by treatment with HSCs. GDNF belongs to the transforming growth factor- β superfamily and was discovered to be a potent neurotrophic factor for midbrain dopaminergic neurons (Lin et al., 1993). GDNF was reported to confer protection to neurons during various types of injury to the nervous system *in vitro* and *in vivo* (Li et al., 1995; Wang et al., 2002). A survival-promoting effect of GDNF on inner ear hair cells against ototoxicity has been reported *in vivo* (Kuang et al., 1999). In our previous report,

we also showed that adenovirus-mediated overexpression of GDNF significantly prevented progressive IHC degeneration after cochlear ischemia in gerbils (Hakuba et al., 2003b). In accordance with these previous reports, we showed that HSCs had the potential to upregulate the GDNF protein level in the organ of Corti after ischemia, suggesting protective effects of GDNF against ischemia-induced hair cell damage. In normal adult rodent, GDNF expression is observed in IHCs (Ylikoski et al., 1998) and the level of GDNF in IHCs was upregulated after noise exposure (Nam et al., 2000). We, then, speculate that cochlear ischemia can upregulate the GDNF level in IHCs and HSCs can modulate the GDNF level in the organ of Corti after ischemia, although further histochemical investigation must be required to confirm this assumption.

CONCLUSION

In conclusion, our study clearly showed that intrascalar injection of HSCs prevented a shift in the ABR threshold and attenuated the progressive IHC damage after cochlear ischemia. In addition, injected HSCs had the potential to upregulate the protein level of GDNF in the organ of Corti after cochlear ischemia. At present, there are some difficulties for the clinical use of HSCs because we can get only a small amount of HSCs from the bone marrow and the technique for proliferating HSCs *ex vivo* is not established yet. Moreover, long-term effects of HSC transplantation are not fully elucidated and unexpected adverse effects such as malignancy and inappropriate immuno-response are not negligible. However, these data suggest that HSC transplantation could be useful in the treatment of SNHL.

Acknowledgment—We are grateful to Ms. K. Hiraoka for her secretarial assistance. The present study was supported in part by a grant-in-aid from the Ministry of Education, Science and Culture, Japan.

REFERENCES

- Alvarez-Dolado M, Pardal R, Garcia-Verdugo JM, Fike JR, Lee HO, Pfeffer K, Lois C, Morrison SJ, Alvarez-Buylla A (2003) Fusion of bone-marrow-derived cells with Purkinje neurons, cardiomyocytes and hepatocytes. *Nature* 425:968–973.
- Askenasy N, Farkas DL (2002) Optical imaging of PKH-labeled hematopoietic cells in recipient bone marrow *in vivo*. *Stem Cells* 20:501–513.
- Brandt A, Striessnig J, Moser T (2003) CaV1.3 channels are essential for development and presynaptic activity of cochlear inner hair cells. *J Neurosci* 23:10832–10840.
- Chopp M, Li Y (2002) Treatment of neural injury with marrow stromal cells. *Lancet Neurol* 1:92–100.
- Crigger L, Robey RC, Asawachaicham A, Gaupp D, Phinney DG (2006) Human mesenchymal stem cell subpopulations express a variety of neuro-regulatory molecules and promote neuronal cell survival and neurogenesis. *Exp Neurol* 198:54–64.
- Gillespie LN, Shepherd RK (2005) Clinical application of neurotrophic factors: the potential for primary auditory neuron protection. *Eur J Neurosci* 22:2123–2133.
- Goodell MA, Brose K, Paradis G, Conner AS, Mulligan RC (1996) Isolation and functional properties of murine hematopoietic stem cells that are replicating *in vivo*. *J Exp Med* 183:1797–1806.
- Hakuba N, Gyo K, Yanagihara N, Mitani A, Kataoka K (1997) Efflux of glutamate into the perilymph of the cochlea following transient ischemia in the gerbil. *Neurosci Lett* 230:69–71.
- Hakuba N, Koga K, Shudou M, Watanabe F, Mitani A, Gyo K (2000) Hearing loss and glutamate efflux in the perilymph following transient hindbrain ischemia in gerbils. *J Comp Neurol* 418:217–226.
- Hakuba N, Matsubara A, Hyodo J, Taniguchi M, Maetani T, Shimizu Y, Tsujiuchi Y, Shudou M, Gyo K (2003a) AMPA/kainate-type glutamate receptor antagonist reduces progressive inner hair cell loss after transient cochlear ischemia. *Brain Res* 979:194–202.
- Hakuba N, Watabe K, Hyodo J, Ohashi T, Eto Y, Taniguchi M, Yang L, Tanaka J, Hata R, Gyo K (2003b) Adenovirus-mediated overexpression of a gene prevents hearing loss and progressive inner hair cell loss after transient cochlear ischemia in gerbils. *Gene Ther* 10:426–433.
- Hata R, Matsumoto M, Hatakeyama T, Ohtsuki T, Handa N, Niinobe M, Mikoshiba K, Sakaki S, Nishimura T, Yanagihara T, Kamada T (1993) Differential vulnerability in the hindbrain neurons and local cerebral blood flow during bilateral vertebral occlusion in gerbils. *Neuroscience* 56:423–439.
- Hata R, Matsumoto M, Matsuyama T, Yamamoto K, Hatakeyama T, Kubo T, Mikoshiba K, Sakaki S, Sugita M, Yanagihara T (1998) Brainstem auditory evoked potentials during brainstem ischemia and reperfusion in gerbils. *Neuroscience* 83:201–213.
- Hyodo J, Hakuba N, Koga K, Watanabe F, Shudou M, Taniguchi M, Gyo K (2001) Hypothermia reduces glutamate efflux in perilymph following transient cochlear ischemia. *Neuroreport* 12:1983–1987.
- Kuang R, Hever G, Zajic G, Yan Q, Collins F, Louis JC, Keithley E, Magal E (1999) Glial cell line-derived neurotrophic factor. Potential for otoprotection. *Ann N Y Acad Sci* 884:270–291.
- Li H, Corrales CE, Edge A, Heller S (2004) Stem cells as therapy for hearing loss. *Trends Mol Med* 10:309–315.
- Li H, Liu H, Heller S (2003a) Pluripotent stem cells from the adult mouse inner ear. *Nat Med* 9:1293–1299.
- Li H, Roblin G, Liu H, Heller S (2003b) Generation of hair cells by stepwise differentiation of embryonic stem cells. *Proc Natl Acad Sci U S A* 100:13495–13500.
- Li L, Wu W, Lin LF, Lei M, Oppenheim RW, Houenou LJ (1995) Rescue of adult mouse motoneurons from injury-induced cell death by glial cell line-derived neurotrophic factor. *Proc Natl Acad Sci U S A* 92:9771–9775.
- Lin LF, Doherty DH, Lile JD, Bektesh S, Collins F (1993) GDNF: a glial cell line-derived neurotrophic factor for midbrain dopaminergic neurons. *Science* 260:1130–1132.
- Maetani T, Hakuba N, Taniguchi M, Hyodo J, Shimizu Y, Gyo K (2003) Free radical scavenger protects against inner hair cell loss after cochlear ischemia. *Neuroreport* 14:1881–1884.
- Mahmood A, Lu D, Chopp M (2004) Intravenous administration of marrow stromal cells (MSCs) increases the expression of growth factors in rat brain after traumatic brain injury. *J Neurotrauma* 21:33–39.
- Masson S, Harrison DJ, Plevris JN, Newsome PN (2004) Potential of hematopoietic stem cell therapy in hepatology: a critical review. *Stem Cells* 22:897–907.
- Morzane I, Hakuba N, Hyodo J, Shimizu Y, Fujita K, Yoshida T, Gyo K (2005) Ischemic damage increases nitric oxide production via inducible nitric oxide synthase in the cochlea. *Neurosci Lett* 391:62–67.
- Nakashima T, Naganawa S, Sone M, Tominaga M, Hayashi H, Yamamoto H, Liu X, Nuttall AL (2003) Disorders of cochlear blood flow. *Brain Res Brain Res Rev* 43:17–28.
- Nam YJ, Stover T, Hartman SS, Altschuler RA (2000) Upregulation of glial cell line-derived neurotrophic factor (GDNF) in the rat cochlea following noise. *Hear Res* 146:1–6.
- Punzel M, Ho AD (2001) Divisional history and pluripotency of human hematopoietic stem cells. *Ann N Y Acad Sci* 938:72–81.
- Roehm PC, Hansen MR (2005) Strategies to preserve or regenerate spiral ganglion neurons. *Curr Opin Otolaryngol Head Neck Surg* 13:294–300.
- Seidman MD, Quirk WS, Shirwany NA (1999) Mechanisms of alterations in the microcirculation of the cochlea. *Ann N Y Acad Sci* 884:226–232.

- Shepherd RK, Roberts LA, Paolini AG (2004) Long-term sensorineural hearing loss induces functional changes in the rat auditory nerve. *Eur J Neurosci* 20:3131–3140.
- Spoendlin H (1967) The innervation of the organ of Corti. *J Laryngol Otol* 81:717–738.
- Takakura N, Watanabe T, Suenobu S, Yamada Y, Noda T, Ito Y, Satake M, Suda T (2000) A role for hematopoietic stem cells in promoting angiogenesis. *Cell* 102:199–209.
- Taniguchi M, Hakuba N, Koga K, Watanabe F, Hyodo J, Gyo K (2002) Apoptotic hair cell death after transient cochlear ischemia in gerbils. *Neuroreport* 13:2459–2462.
- Tateya I, Nakagawa T, Iguchi F, Kim TS, Endo T, Yamada S, Kageyama R, Naito Y, Ito J (2003) Fate of neural stem cells grafted into injured inner ears of mice. *Neuroreport* 14:1677–1681.
- Wang X, Willenbring H, Akkari Y, Torimaru Y, Foster M, Al-Dhalimy M, Lagasse E, Finegold M, Olson S, Grompe M (2003) Cell fusion is the principal source of bone-marrow-derived hepatocytes. *Nature* 422:897–901.
- Wang Y, Chang CF, Morales M, Chiang YH, Hoffer J (2002) Protective effects of glial cell line-derived neurotrophic factor in ischemic brain injury. *Ann N Y Acad Sci* 962:423–437.
- Watanabe F, Koga K, Hakuba N, Gyo K (2001) Hypothermia prevents hearing loss and progressive hair cell loss after transient cochlear ischemia in gerbils. *Neuroscience* 102:639–645.
- Ylikoski J, Pirvola U, Virkkala J, Suvanto P, Liang XQ, Magal E, Altschuler R, Miller JM, Saarna M (1998) Guinea pig auditory neurons are protected by glial cell line-derived growth factor from degeneration after noise trauma. *Hear Res* 124:17–26.

(Accepted 23 December 2006)
(Available online 22 February 2007)



Ginsenoside Rb1 protects against damage to the spiral ganglion cells after cochlear ischemia

Kensuke Fujita^a, Nobuhiro Hakuba^{a,*}, Ryuji Hata^b, Isao Morizane^a, Tadashi Yoshida^a,
Masachika Shudou^c, Masahiro Sakanaka^b, Kiyofumi Gyo^a

^a Department of Otolaryngology, Ehime University School of Medicine, Ehime, Japan

^b Integrated Basic Medical Science, Division of Functional Histology, Ehime University School of Medicine, Ehime, Japan

^c Central Research Laboratory, Ehime University School of Medicine, Ehime, Japan

Received 10 August 2006; received in revised form 22 December 2006; accepted 3 January 2007

Abstract

The effects of transient cochlear ischemia on spiral ganglion cells (SGCs) were studied in Mongolian gerbils. Ischemic insult was induced by occluding the bilateral vertebral arteries of gerbils for 15 min. Seven days after ischemia, the percentage of SGCs decreased to 67.5% from the preischemic baseline in the basal turn. Evaluation with immunohistochemical staining showed TUNEL-positive reactions in the SGCs with fragmented nuclei. In addition, we investigated the protective effects of ginsenoside Rb1 (gRb1) against ischemic injury to SGCs. Seven days after ischemia, the auditory brainstem response threshold shift was significantly reduced and the percentage of SGCs decreased to 90.2% from the preischemic baseline in the basal turn in the gRb1-treated group. These findings suggest that gRb1 prevented hearing loss caused by ischemic injury to SGCs in Mongolian gerbils.

© 2007 Elsevier Ireland Ltd. All rights reserved.

Keywords: Transient cochlear ischemia; Spiral ganglion cells; Ginsenoside Rb1; TUNEL staining; Bcl-xL protein

Ischemic injury is a major cause of acute sensorineural hearing loss [1,2,8]. We thus evaluated the pathology of transient cochlear ischemia in Mongolian gerbils. In these animals, the posterior cerebral communicating arteries are lacking and the labyrinthine arteries are nourished solely by the vertebral arteries. We previously showed that inner hair cells are more vulnerable to damage via the apoptotic process than outer hair cells and that transient ischemia for 5 min caused delayed cell death in the spiral ganglion [3,5,9,15,16]. However, the mechanism of neuronal damage to spiral ganglion cells (SGCs) has not been clarified.

Ginseng root is widely prescribed in Asian countries for a variety of ailments. Ginsenoside Rb1 (gRb1) is the main ingredient of ginseng root. In the brain, gRb1 has been shown to prevent apoptotic cell death via regulation of the Bcl-xL protein, which inhibits apoptosis by preventing the release of cytochrome *c* in the cell death pathway [17]. In the present study, we investigated the effects of transient cochlear ischemia on SGCs and evalu-

ated whether postischemic intravenous infusion of gRb1 in this setting could prevent SGC degeneration.

The following study was conducted in accordance with the Guidelines for Animal Experimentation of Ehime University School of Medicine, Japan. Adult male Mongolian gerbils weighing 60–80 g were used as subjects. Transient cochlear ischemia was induced in the animals by temporarily occluding the vertebral arteries bilaterally in the neck, as described by Hata et al. [4].

The hearing ability of animals treated with gRb1 was assessed by sequential recording of ABR. Measurements were made before and 4 and 7 days ($n = 6$ each) after the ischemia insult. The ABR in response to an 8000-Hz tone burst (0.5-ms rise/fall time and 10-ms duration) was measured using a signal processor (NEC Synax 1200; NEC Medical Systems, Tokyo, Japan). This frequency was selected because we previously found that the higher-frequency region of the cochlea was more vulnerable to ischemic injury than the middle or lower-frequency regions [9]. The average ABR thresholds in control and gRb1-treated group were analyzed using a two-tailed Mann–Whitney *U*-test.

Ginsenoside Rb1 was isolated and purified from the crude saponin fraction in the rhizome of Korean red ginseng (*Panax*

* Corresponding author. Tel.: +81 89 960 5366; fax: +81 89 960 5368.

E-mail address: hakubax@ehime-u.ac.jp (N. Hakuba).

ginseng, C.A. Meyer) by repeated-column chromatography on silica gel with $\text{CHCl}_3\text{--MeOH--H}_2\text{O}$ (65:35:10) and on octadecylsilyl (ODS) silica with $\text{MeOH--H}_2\text{O}$ (1:1–7:3) [12]. GRb1 was then dissolved in isotonic saline. A total of 200 μL of gRb1 solution (50 $\mu\text{g}/200 \mu\text{L}$) was injected into the left femoral veins of the gRb1 group ($n=3$) and 200 μL of saline was injected into the left femoral veins of the control group ($n=3$) 1 h after ischemia.

To determine SGC survival, the six gerbils were anesthetized deeply, killed 7 days after ischemia, and fixed by cardiac perfusion (4% paraformaldehyde in phosphate buffer). After decalcification in EDTA and embedding in paraffin, 6- μm sections were cut from the gerbils in a paramodiolar plane. Every fourth section was mounted on a glass slide and stained with hematoxylin–eosin. Six sections were randomly selected from the 10 most mid-modiolar sections from each animal and used in the quantitative analysis of the SGCs. Counting was performed in a double-blind fashion. All neurons meeting the size and shape criteria to be considered type I SGCs within each profile of Rosenthal's canal in the basal turn were counted. The outline of the Rosenthal's canal profile was then traced to generate a SGC density, expressed as the density of SGC in an area of 10,000 μm^2 . The baseline average number of SGCs was counted in six animals without ischemia. This baseline average was used to calculate the percentage of lost SGCs 7 days after ischemia. Statistical assessment of the differences in the SGC densities between the study groups was performed with analysis of variance and Student's *t*-test.

Double-stranded DNA breaks were detected by terminal deoxynucleotidyl transferase-mediated dUTP-biotin nick end-labeling (TUNEL) using specimens from six gerbils 1 day after ischemia. An apoptosis in situ detection kit (Roche, Mannheim, Germany) was used for the TUNEL staining. Deparaffinized sections were washed with distilled water and treated with proteinase K for 5 min at 37 °C. After washing three times with 0.01 M phosphate-buffered saline (PBS), the sections were treated with TdT solution for 10 min at 37 °C. To block endogenous peroxidase activity, the sections were treated with 3% hydrogen peroxide for 5 min at room temperature. Peroxidase-conjugated antibody was applied for 10 min at 37 °C. After washing with 0.01 M PBS, nick end-labeling was visualized with 3,3'-diaminobenzidine (DAB) solution.

For the Bcl-xL immunostaining, six gerbils were used 1 day after ischemia. The sections from both the gRb1 and control groups were deparaffinized and exposed to 5% normal horse serum (NHS) in PBS for 1 h. The sections were subsequently incubated for 12 h with rabbit anti-Bcl-xL antibody (1:2000 dilution; Santa Cruz Biotechnology, Santa Cruz, CA, USA), flooded for 1 h with biotin-conjugated goat anti-rabbit immunoglobulin (1:400 dilution; DAKO Cytomation Co., Kyoto, Japan) in 1% NHS–PBS, and incubated in biotinylated tyramine solution containing 0.01% H_2O_2 . The sites of bound primary antibodies were visualized after incubating the sections with ABC reagent (Vector Laboratories, Burlingame, CA, USA). Sections from each animal were immunostained in the same run for between-group comparisons.

The fine structure of the SGCs was evaluated with transmission electron microscopy (TEM). Four animals were killed 1 day after ischemia. Immediately following removal of both otic bullae during deep anesthesia, the cochleae were perfused with 2.5% glutaraldehyde. The cochleae were then removed, immersed for 8 h in the same fixative at 4 °C, and dissected in PBS (pH 7.4). Pieces of the organ of Corti were used for whole-mount staining and TEM analysis. The specimens were postfixed with 2% osmium tetroxide for 1 h at room temperature. Following dehydration, the specimens were embedded in epoxy resin. Sections were cut with an ultramicrotome and stained with uranyl acetate and lead citrate. The cochleae were then observed with a TEM (H300; Hitachi, Tokyo, Japan).

The average increase in the ABR threshold was 22.5 ± 2.9 dB on the seventh day after inducing ischemia with saline treatment. In contrast, the ABR threshold increased to 14.2 ± 3.8 dB in ischemic animals treated with gRb1. The average increase in the ABR threshold 7 days after inducing ischemia was significantly lower in animals treated with gRb1 than in saline-treated animals ($P < 0.05$) (Fig. 1).

Fig. 2 shows the representative sections of Rosenthal's canal in the base of the cochlea from a control subject (Fig. 2a) and a gRb1-treated subject (Fig. 2b). Seven days after ischemia, the mean percentage decrease in SGCs was 30.6 ± 2.1 , 16.0 ± 7.8 , and $7.5 \pm 1.8\%$ at the basal, second, and apical turns, respectively. These results show that SGCs at the basal turn were more vulnerable than those at the second and apical turns. Therefore, we investigated the effect of gRb1 on ischemic damage to SGCs in the basal turn.

Before ischemia, the average number of SGCs in the basal turn was $28.1/10,000 \mu\text{m}^2$. Seven days after ischemia, the average number of SGCs in the basal turn was $25.8/10,000 \mu\text{m}^2$ in the gRb1 group and $19.3/10,000 \mu\text{m}^2$ in the control group. The mean percentage loss of SGCs in the gRb1 group was $8.0 \pm 4.7\%$, which was significantly smaller than the $30.6 \pm 2.1\%$ loss observed in the control group ($P < 0.05$; Fig. 3). Injection of gRb1 resulted in enhanced survival of SGCs 7 days after ischemia.

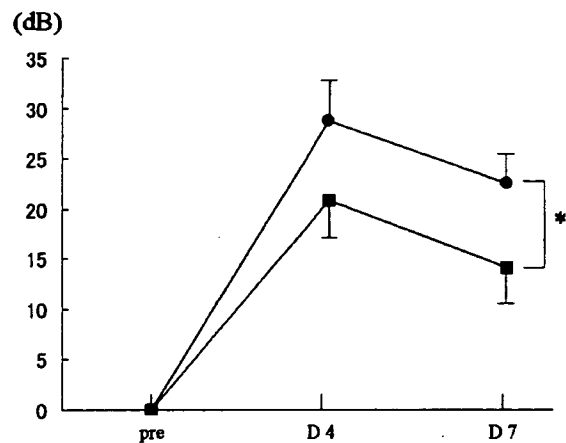


Fig. 1. Changes in the auditory brainstem response (ABR) threshold following transient cochlear ischemia. The ABR was measured in response to an 8000-Hz tone burst. The ABR threshold before ischemia was defined as 0 dB. * $P < 0.05$ vs. the control.

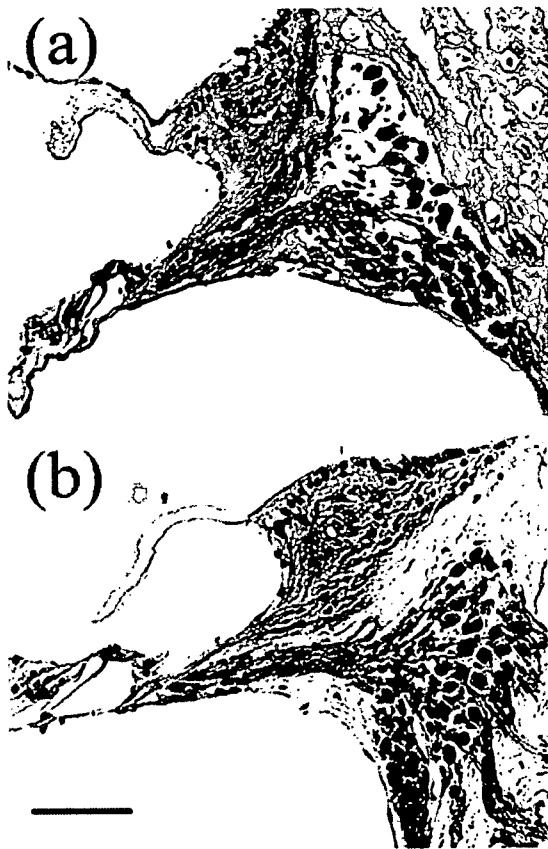


Fig. 2. Representative sections of Rosenthal's canal in the base of the cochlea from a control subject (a) and a gRb1-treated subject (b). A clear difference was observed in the survival of these subjects. Scale bar = 60 μ m.

Ischemia induced TUNEL-positive reactions in SGCs with fragmented nuclei (Fig. 4a). Few TUNEL-positive cells were observed in the basal turn of the cochleae in animals administered gRb1 (Fig. 4b). The mean percentage of TUNEL-positive cells in the specimens 1 day after ischemia was $24.4 \pm 7.8\%$ for animals treated with saline and $4.1 \pm 2.9\%$ for animals treated with gRb1.

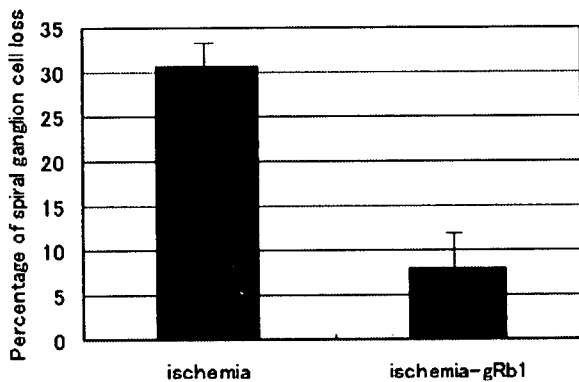


Fig. 3. The percentage decrease of SGCs in the basal turn 7 days after ischemic injury. SGC degeneration was significantly lower in the gRb1-treated group compared to the control group ($P < 0.01$).

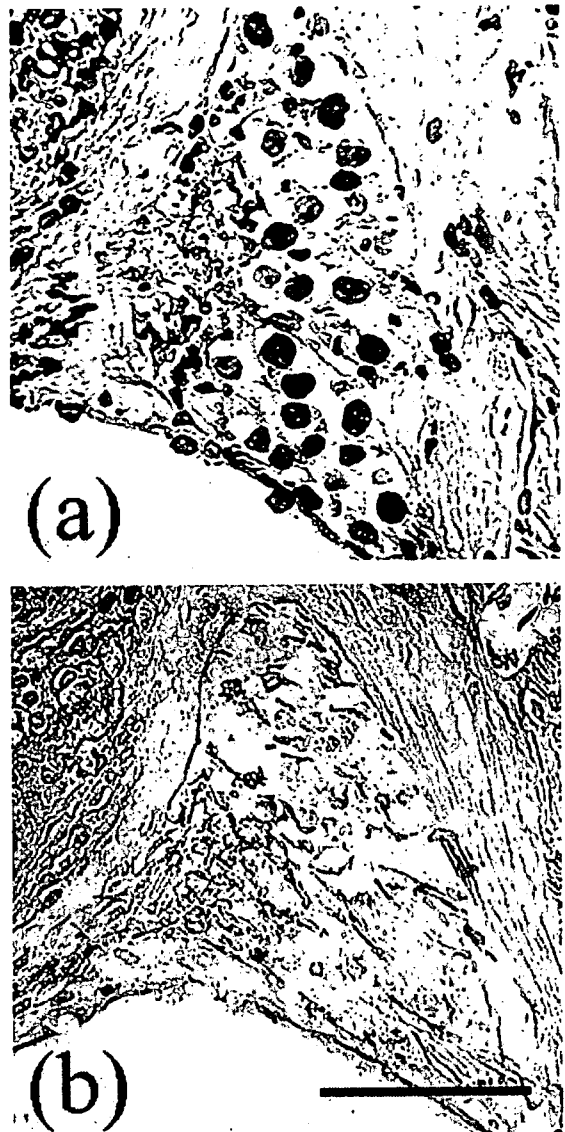


Fig. 4. Light microscopic photograph of TUNEL staining in the spiral ganglion. TUNEL-positive cells were observed in the spiral ganglion of control animals (a), whereas no TUNEL-positive cells were observed in gRb1-treated animals (b). Scale bar = 60 μ m.

After Bcl-xL immunostaining, strongly stained cells were present throughout the basal turn in the gRb1 group (Fig. 5c). Weak immunopositive cells were detected in the control group (Fig. 5b) or in specimens not exposed to the antibodies (data not shown). The results of the immunostaining for Bcl-xL were classified by two evaluators, who were blind to the treatment the animals had received, into four categories: no, mild, moderate, and strong staining. Table 1 summarizes the results of the immunostaining for Bcl-xL into four categories.

The ultrastructure of the SGCs was analyzed in the cochlear sections. Under electron microscopy, we observed the appearance of nuclear fragmentation and irregularly shaped nuclei in the control group (Fig. 6a), whereas most of the cells in the gRb1-treated group had regularly shaped nuclei (Fig. 6b). We further

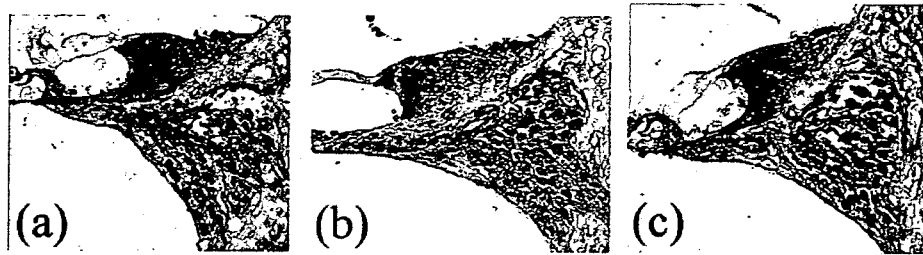


Fig. 5. Immunostaining for Bcl-xL before ischemia (a), 1 day after ischemia in the spiral ganglion of controls (b) and gRb1-treated animals (c). Ginsenoside Rb1 increased the expression of Bcl-xL 1 day after ischemia in the spiral ganglion. Scale bar = 60 μ m.

Table 1
Summary of immunostaining for Bcl-xL

Control	Day 1	Day 1 + gRb1
++	+	++ to +++

+: mild staining; ++: moderate staining; +++: strong staining; +gRb1: animals given ginsenoside Rb1; control: before the induction of ischemia; Day 1: 1 day after the induction of ischemia.

distinguished SGCs as types I and II under electron microscopy. Dysmorphic nuclei were observed in 36.9% of type I SGCs and 18.5% of type II SGCs. We postulate that type I SGCs were more vulnerable than type II SGCs.

As primary auditory neurons, SGCs play an important role in hearing. In patients with severe sensorineural hearing loss, the

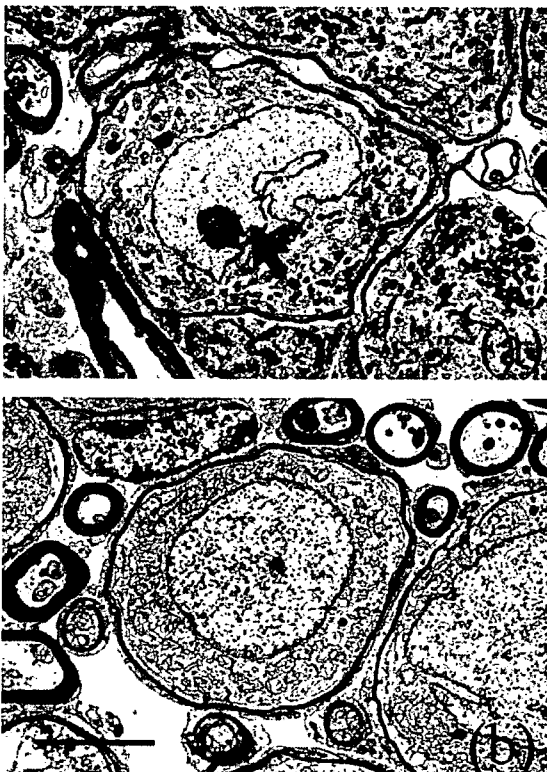


Fig. 6. Electron micrographs of the spiral ganglion 1 day after ischemia in controls (a) and gRb1-treated animals (b). (a) The SGC of the control animal has an indented nucleus with condensed chromatin (arrow). (b) The SGC of the gRb1-treated animal appears normal. Scale bar = 5 μ m.

only therapeutic intervention is a cochlear implant, which electrically stimulates residual primary auditory neurons to provide the patients with auditory cues required for speech perception. Most studies in humans and animals have shown that spiral ganglion neurons are lost following the loss of hair cells, particularly as a result of ototoxic drugs, noise exposure, and aging [6,7,11]. Results from these studies suggest that degeneration of the auditory nerve is a slow process that occurs over months or years. In contrast, the application of ouabain, which binds to Na^+ , K^+ -ATPase and blocks its activity in the cochlea, has been reported to result in a rapid loss of SGCs via apoptotic cell death [10,13]. However, the mechanism of ischemic injury has not been elucidated. We induced ischemic injury in gerbils for 15 min and observed an agglomeration of chromatin and aberrant nuclei via electron microscopy 1 day after ischemia. Additionally, apoptotic cells were detected by the TUNEL method. These findings indicate that ischemic injury is caused by apoptotic cell death in SGCs. The percentage of SGCs decreased to 68.5% from the preischemic baseline in the basal turn 7 days after ischemic injury. This is the first study to report how ischemic injury induces apoptotic cell death in SGCs and the degree of degeneration that ensues.

Ginseng root is an important component of treatment in many Asian countries and consists of two major ingredients: crude ginseng saponin and nonsaponin fractions. To date, more than 40 saponins have been isolated from ginseng root and identified chemically. The saponins can be classified into three major groups according to their chemical structures: protopanaxadiol, protopanaxatriol, and oleanolic acid. Ginsenoside Rb1, ginsenoside Rg1, and ginsenoside Ro are representative substances [14]. Zhang et al. reported that gRb1 rescued cortical neurons in the ischemic penumbra and reduced the cortical infarct volume by approximately 50%. Their report demonstrated that gRb1 deregulated the expression of Bcl-xL, which is known to suppress activation of procaspase-9 by forming a complex with Apaf-1. This, in turn, prevents the release of cytochrome c from mitochondria, thereby maintaining cell viability and cell survival [17]. In the present study, postischemic administration of gRb1 preserved the configuration of the spiral ganglion and decreased the number of TUNEL-positive cells with obvious expression of Bcl-xL 1 day after ischemia. We postulated that gRb1 may suppress apoptotic cell death in SGCs by activating the Bcl-xL signaling pathway. We observed decreased degeneration of SGCs in the basal turn of gRb1-treated animals 7 days after ischemia compared to untreated controls. Our results suggest